Technical University of Denmark

DTU

Bragg grating induced cladding mode coupling due to asymmetrical index modulation in depressed cladding fibers

Berendt, Martin Ole; Grüner-Nielsen, Lars Erik; Soccolich, C.F.; Bjarklev, Anders Overgaard

DTU Library
Technical Information Center of Denmark

measured phase delay error for a similar but apodized grating. As expected, apodization decreased the ripples.

Although this technique was demonstrated on short commercial gratings, it is better suited to resolve the phase ripples in long dispersion-compensating gratings.

1. S. Barcelos *et al.*, Electron. Lett. **31**, 1280 (1995).
2. M. Volanthen *et al.*. Electron. Lett. **32**, 757 (1996).
3. K. Takiguchi *et al.*, IEEE Photon. Technol. Lett. **6**, 86 (1994).
4. K. Ennser *et al.*, presented at European Conference on Optical Communication (ECOC'97), Edinburgh, Scotland, 1997.
5. G.H. Smith *et al.*, Electron. Lett. **33**, 74 (1997).

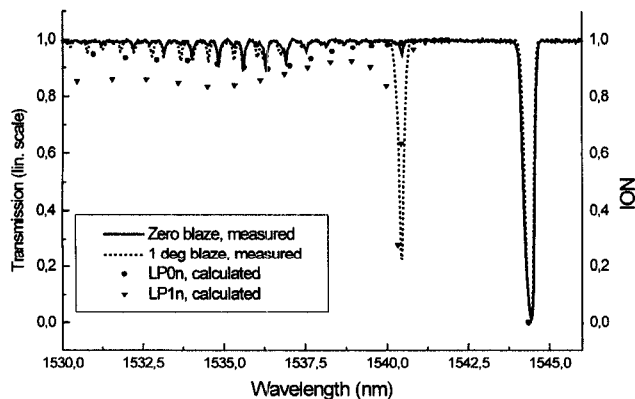## TuA6   12:15pm

Bragg grating induced cladding mode coupling due to asymmetrical index modulation in depressed cladding fibers

Martin O. Berendt, Lars Grüner-Nielsen,* Carl E. Soccolich,**
Anders Bjarklev, *Department of Electromagnetic Systems,
EMI, DTU Building 348, DK-2800 Lyngby, Denmark;
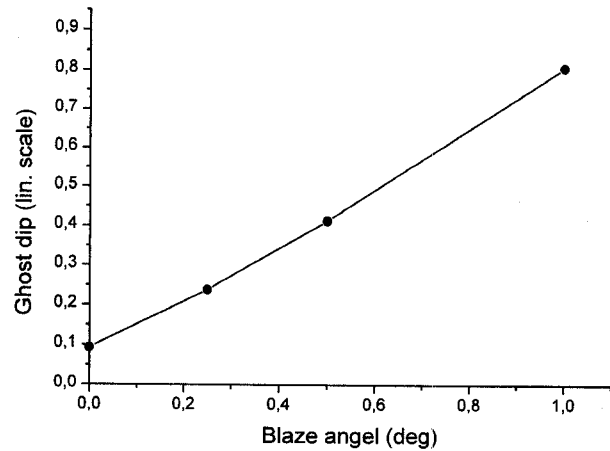E-mail: mob@emi.dtu.dk*

UV-written Bragg gratings find wide spread use as wavelength selective components. In reflection high extinction ratios is routinely obtained. However, coupling to cladding modes gives excess loss on the short wavelength side of the main reflection. Different fiber-designs have been proposed to reduce this problem.[1-3] Neither of these designs seems to give complete solutions. In particular, the otherwise promising depressed cladding design gives a pronounced coupling to one LP_{1n} mode, this has been referred to as a Ghost grating.[4]

To find the modes of the fiber we have established a numerical modesolver based on the staircase-approximation method. The Bragg grating causes coupling between the fundamental LP_{01} mode and higher order LP_{1p} modes that satisfy phasematching. The coupling strength is determined by the overlap integral of the LP_{01}, the LP_{1p} mode, and the UV-induced index perturbation. For LP_{0n} the index perturbation is set to one in the core and zero elsewhere. For LP_{1n} it is simplified to the worst case, *i.e.*, opposite sign of the field.
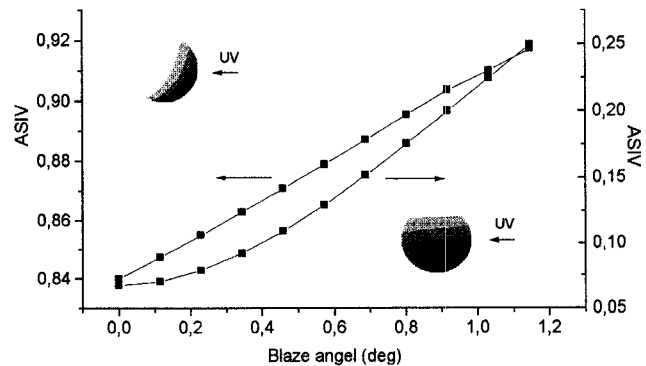
Figure 1 shows measured transmission spectres along with normalized overlap integrals (NOI) calculated for the fiber index profile. The fiber used has a high core index $(15 \cdot 10^{-3})$ and a depressed cladding ring

TuA6   **Fig. 2.**   Measured Ghost dip relative to Bragg dip as a function of blaze angle.

TuA6   **Fig. 3.**   Asymmetrical index volume (ASIV) as a function of blaze angel, left trace: 800 dB/mm; right trace: 50 dB/mm (note zero slope for zero blaze). Insert shows distribution of UV-induced index perturbation in a fiber cross section.

of depth $-5 \cdot 10^{-3}$ and width 5 μm. To fit the measured spectrum the depth of the cladding ring was set to $-6 \cdot 10^{-3}$.

At 1°, blaze of the phasemask a large dip is seen 4 nm from the Bragg wavelength. This corresponds to the calculated LP_{16}, LP_{17} cladding modes. Changing the depth and width of the depressed cladding ring shifts the Ghost dip to other mode numbers but the size and spectral position is virtually unaltered. When the blaze is reduced to $0° \pm 0.02°$ this dip is reduced to six percent of the Bragg dip. This behavior was further investigated by writing four gratings under identical conditions except for blaze angles [(Fig. 2)].

The UV-induced index change was deduced assuming cosine squared longitudinal index modulation, blaze angel θ and exponential attenuation (coefficient γ) of the UV-beam entering the fiber core from the side;

$$n_{UV}(r,\phi,z,\theta) = n_{UV\,max} \cdot \exp(-\gamma(\sqrt{a^2 - (r \cdot \sin(\phi))^2} + r \cdot \cos(\phi))) \cdot \alpha_{Blaze}(r,\phi,z,\theta)$$

$$\alpha_{Blaze}(r,\phi,z,\theta) = \frac{a - r \cdot \sin(\phi)}{2a} \cos^2\left(\frac{\pi}{\Lambda} \cdot z\right) + \frac{a + r \cdot \sin(\phi)}{2a} \cos^2\left(\frac{\pi}{\Lambda}\left(z - \frac{2a}{\tan(\theta)}\right)\right),$$

TuA6   **Fig. 1.**   Measured cladding mode coupling spectra and calculated NOI.

where $n_{UV\,max}$ is the maximum UV-induced index change, Λ is the grating period and a is the core radius.

The volume integral of n_{UV} subtracted a cosine squared index modulation is proportional to the NOI, assuming no radial field variation and step azimuthal variation, in the core. This integral we denote as the asymmetrical index volume (ASIV).

The analysis indicate two regimes [(Fig. 3)], namely a blaze-dominated LP_{1n} coupling for small UV attenuation (<100 dB/mm) and a side illumination dominated behavior for large UV attenuation. The measurement in Fig. 2 seems to fall in between these extremes. For the fiber used, we estimate an UV attenuation of 400 dB/mm. Comparing this result with the residual Ghost dip for zero blaze and published measurements of index profiles after UV-sidewriting,[5] we conclude that asymmetry arising from side illumination is very important for the understanding of LP_{1n} coupling. Design of fibers and writing setups, with the aim of reducing cladding mode coupling must be based on this new understanding.

*Lucent Technologies Specialty Fiber Devices, Priorparken 680, DK-2605 Brøndby, Denmark
**Lucent Technologies Specialty Fiber Devices, 700 Mountain Avenue, Murray Hill, New Jersey

1. T. Komukai and M. Nakazawa, in Proceedings of European Conference on Optical Communication (ECOC'95), 1995, pp. 31–34.
2. E. Delevaque, S. Boj, J.F. Bayon, H. Poignant, J. Le Mellot, M. Monerie, P. Niay, P. Bernage, in Optical Fiber Communication Conference, Vol. 8 of 1995 OSA Technical Digest Series (Optical Society of America, Washington, D.C., 1995), postdeadline paper PD5.
3. L. Dong, L. Reekie, J.L. Cruz, J.E. Capelen, D.N. Payne, in Proceedings of European Conference on Optical Communication (ECOC'96), 1996, pp. 1.53–1.56.
4. S.J. Hewlet, J.D. Love, G. Meltz, T.J. Basily, W.W. Morey, Electron. Lett. **31**, 820–822 (1995).
5. A. Vengsarkar, Q. Zhong, D. Inniss, W.A. Reed, P. Lemaire, S.G. Kosinski, Opt. Lett. **19**, 1260–1262 (1994).

TuB

11:00am–12:30pm

Room A2

Vertical Cavity Surface-Emitting Lasers

Connie J. Chang-Hasnain, *University of California–Berkeley, Presider*

**TuB1 (Invited)**   **11:00am**

Fusion bonding for vertical-cavity surface-emitting lasers

Dubravko Babić, *Hewlett-Packard Laboratories, Palo Alto, California, 94304; E-mail: babic@hpl.hp.com*

This talk summarizes current efforts in fusion bonding and the application of this technology to vertical-cavity surface-emitting lasers at Hewlett-Packard Laboratories. We discuss electrical characteristics, carrier-concentration profiling and SIMS analyses through InP/GaAs junctions, and the development of 1300 nm VCSELs.
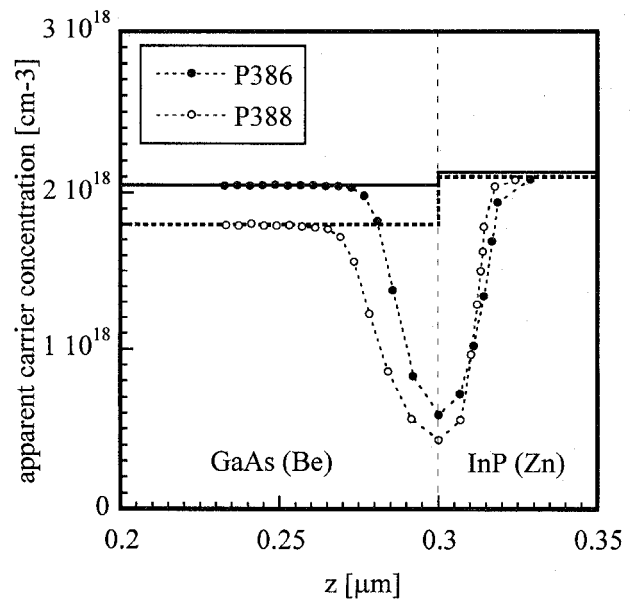
TuB1   Fig. 1.   Apparent hole concentration profile in a p-GaAs/p-InP fused junction.
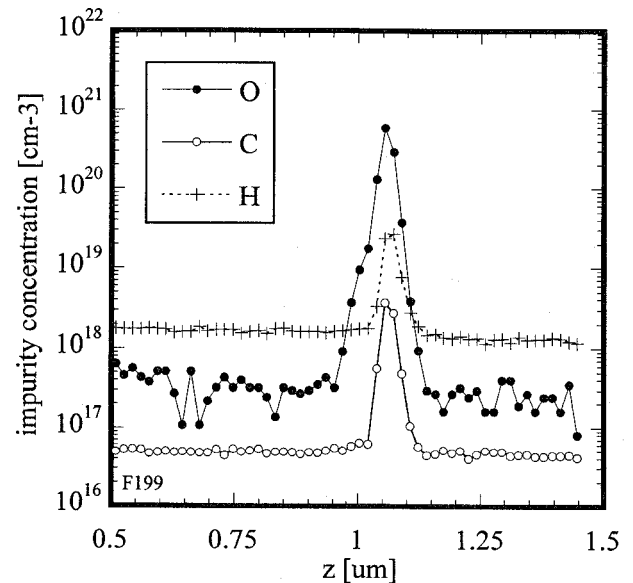
TuB1   Fig. 2.   SIMS profile through a p-InP/n-GaAs fused junction.